Published in final edited form as:
Exp Eye Res. 2010 May ; 90(5): 572–582. doi:10.1016/j.exer.2010.02.001.

Pax6a and Pax6b are required at different points in neuronal progenitor cell proliferation during zebrafish photoreceptor regeneration

Ryan Thummel[1], **Jennifer M. Enright**, **Sean C. Kassen**, **Jacob E. Montgomery**, **Travis J. Bailey**, and **David R. Hyde**[*]
Department of Biological Sciences and the Center for Zebrafish Research University of Notre Dame, Notre Dame, Indiana, 46556, USA

Abstract

The light-damaged zebrafish retina results in the death of photoreceptor cells and the subsequent regeneration of the missing rod and cone cells. Photoreceptor regeneration initiates with asymmetric Müller glial cell division to produce neuronal progenitor cells, which amplify, migrate to the outer nuclear layer (ONL), and differentiate into both classes of photoreceptor cells. In this study, we examined the role of the Pax6 protein in regeneration. In zebrafish, there are two Pax6 proteins, one encoded by the *pax6a* gene and the other encoded by the *pax6b* gene. We intravitreally injected and electroporated morpholinos that were complementary to either the *pax6a* or *pax6b* mRNA to knockdown the translation of the corresponding protein. Loss of Pax6b expression did not affect Müller glial cell division, but blocked the subsequent first cell division of the neuronal progenitors. In contrast, the paralogous Pax6a protein was required for later neuronal progenitor cell divisions, which maximized the number of neuronal progenitors. Without neuronal progenitor cell amplification, proliferation of resident ONL rod precursor cells, which can only regenerate rods, increased inversely proportional to the number of INL neuronal progenitor cells. This confirmed that Müller glial-derived neuronal progenitor cells are necessary to regenerate cones and that distinct mechanisms selectively regenerate rod and cone photoreceptors. This work also defines distinct roles for Pax6a and Pax6b in regulating neuronal progenitor cell proliferation in the adult zebrafish retina and increases our understanding of the molecular pathways required for photoreceptor cell regeneration.

Keywords

Pax6; morpholino; Müller glia; neuronal progenitor; retina; cell migration; stem cell

*Correspondence should be addressed to: David R. Hyde, Ph.D., Department of Biological Sciences and the Center for Zebrafish Research, University of Notre Dame, Notre Dame, Indiana, 46556, USA, Phone: 1-(574) 631-8054, Fax: 1-(574) 631-7413, dhyde@nd.edu.
[1]Present address: Department of Anatomy and Cell Biology and Department of Ophthalmology Wayne State University School of Medicine, Detroit, MI, 48201, USA

INTRODUCTION

The zebrafish retina undergoes persistent neurogenesis throughout its life (Marcus et al., 1999; Otteson et al., 2001; Otteson and Hitchcock, 2003; Raymond et al., 2006). All retinal neurons, except rods, are derived from a population of neuronal stem cells located at the circumferential marginal zone (Marcus et al., 1999; Raymond et al., 2006). Rods are generated from a limited number of Müller glial cells that divide asymmetrically to produce a neuronal progenitor cell that migrates to the ONL (Bernardos et al., 2007; Raymond et al., 2006). Upon reaching the ONL, this cell is called a rod precursor cell because it is committed to differentiating into a rod photoreceptor (Hitchcock and Raymond, 2004; Morris et al., 2008a; Otteson et al., 2001; Raymond et al., 2006). These rod precursor cells continue to proliferate at a low rate until they differentiate into rods. While a variety of genes are differentially expressed in the neuronal progenitor and rod precursor cells (Hitchcock and Raymond, 2004; Morris et al., 2008b; Otteson et al., 2001; Raymond et al., 2006; Stenkamp, 2007), it is the spatial location that most accurately defines and distinguishes these two cell types at the present time.

A variety of insults to the zebrafish retina induces neuronal death, followed by a significant increase in the number of proliferating Müller glia to produce neuronal progenitors that continue to undergo cell division and accurately differentiate into the lost neurons (Bernardos et al., 2007; Braisted et al., 1994; Cameron, 2000; Fausett and Goldman, 2006; Fimbel et al., 2007; Hitchcock et al., 1992; Maier and Wolburg, 1979; Raymond et al., 2006; Vihtelic and Hyde, 2000; Wu et al., 2001; Yurco and Cameron, 2005). While this regeneration response is largely absent in mammalian retinas (Bringmann et al., 2006), a number of reports indicate that mammalian Müller glia possess features that are similar to adult neuronal stem cells (Lawrence et al., 2007; Rowan and Cepko, 2004). Elucidating the molecules that regulate these proliferative events in a robustly regenerating species could lead to therapies for retinal degenerative diseases.

Constant intense light treatment of dark-adapted *albino* zebrafish selectively kills rod and cone photoreceptors (Vihtelic and Hyde, 2000), which induces approximately 50% of the Müller glia to divide and produce neuronal progenitor cells (Thummel et al., 2008b). These neuronal progenitors initiate expression of stem/progenitor cell markers, including Pax6, Rx1, and Chx10 (Raymond et al., 2006; Thummel et al., 2008a), continue to proliferate, and migrate from the inner nuclear layer (INL) to the outer nuclear layer (ONL). There they ultimately differentiate into rods and cones to replace the lost photoreceptors (Vihtelic and Hyde, 2000). While Ascl1a and Stat3 have been shown to be required for Müller glial proliferation (Fausett et al., 2008; Kassen et al., 2010), there are currently no known molecules that specifically regulate the subsequent proliferation of the neuronal progenitor cells.

Pax6 plays a pivotal role in eye development in species as diverse as flies, zebrafish, mice, and humans (Nornes et al., 1998; Xu et al., 2007). Pax6 is also expressed in the neuronal progenitor cells during regeneration of the adult zebrafish retina (Raymond et al., 2006; Thummel et al., 2008a). Zebrafish possess two paralogous *pax6* genes (*pax6a* and *pax6b*), which encode functionally redundant proteins that regulate formation and differentiation of the retina and lens (Blader et al., 2004). However, neither the redundancy nor the function of the Pax6 paralogs has been investigated in the regenerating retina.

We demonstrated that conditional knockdown of either Pax6a or Pax6b protein expression disrupted discrete events during retinal regeneration. Knockdown of Pax6b expression inhibited the subsequent division of the Müller glia-derived INL neuronal progenitor. In contrast, reduction of Pax6a expression allowed this initial neuronal progenitor cell division,

but it prevented later cell divisions. The reduced number of INL neuronal progenitor cells in both Pax6 knockdown retinas resulted in a corresponding loss of regenerated cones, but not rods. This indicated that Müller glia-derived INL progenitors were required for cone cell regeneration, while rods regenerated from increased amplification of resident ONL rod precursors. This work describes a novel Pax6-dependent mechanism to regulate the extent of neuronal progenitor cell amplification.

MATERIALS AND METHODS

Fish maintenance

Wild-type AB and *albino* strains of zebrafish (*Danio rerio*) were maintained in the Center for Zebrafish Research at the University of Notre Dame Freimann Life Science Center. The adults used for these studies were 6 to 12 months old and 4 to 5 cm in length. Fish were fed brine shrimp and flake food three times daily and maintained under a daily light cycle of 14 hours light (250 lux):10 hours dark at 28.5°C (Detrich et al., 1999; Westerfield, 1995). All protocols used in this study were approved by the animal use committee at the University of Notre Dame and are in compliance with the ARVO statement for the use of animals in vision research.

Morpholinos

This study utilized five lissamine-tagged morpholinos (Gene Tools LLC, Philomath, OR). The Gene Tools Standard Control morpholino (5’ – CCTCTTACCTCAGTTACAATTTATA – 3’) was used as a non-specific control, because it has no complementary sequence in the zebrafish genome. Two different anti-*pax6* morpholinos were used that were based on the previously published anti-*pax6a* and anti-*pax6b* morpholino sequences (Blader et al., 2004). The anti-*pax6a* morpholino is complementary to the 5' UTR of only the *pax6a* mRNA (5’ – TTTGTATCCTCGCTGAAGTTCTTCG – 3’) and the anti-*pax6b* morpholino is complementary to the 5' UTR of only the *pax6b* mRNA (5’ – CTGAGCCCTTCCGAGCAAAACAGTG – 3’). Two 5-base mismatch control morpholinos were derived from the anti-*pax6a* and anti-*pax6b* sequences, 5mis *pax6a* MO-1 (5’ – TTTCTATGCTCGCTCAACTTGTTCG-3’) and 5mis *pax6b* MO-2 (5’ – CTCAGACCTTCCGAGCCAAATACTG – 3’), respectively, with the mismatched bases underlined. Morpholinos were resuspended in water to a working concentration of 3 mM.

Immunoblot of Pax6 expression in morphant zebrafish embryos

Morpholinos were micro-injected into 1–4 cell stage embryos and protein was isolated for immunoblot analysis as previously described (Thummel et al., 2008b). Embryos were injected with either the *anti-pax6a* morpholino, the *anti-pax6b* morpholino, or a cocktail of both morpholinos. Total protein was isolated from uninjected and morphant embryos at 48 hours post fertilization (hpf). Total protein equivalent of 1 embryo was combined with 4x sample buffer and 10x reducing buffer (Invitrogen, Carlsbad, CA), incubated at 70°C for 10 min, and loaded onto a 4–12% SDS-PAGE (Invitrogen). Following electrophoresis, the sample was transferred to a PVDF membrane (Amersham, Pittsburgh, PA). The membrane was blocked in PBS/5% nonfat dry milk/0.1% Tween-20 and then incubated with a rabbit polyclonal anti-Pax6 antiserum (diluted 1:5000, Covance, Berkeley, CA) overnight at 4°C in blocking buffer. The anti-Pax6 antiserum recognizes both zebrafish Pax6 proteins. The membrane was washed in PBS/0.1% Tween-20, and then incubated with an anti-rabbit HRP-conjugated secondary antibody (diluted 1:10,000, Amersham). The ECL-Plus system (Amersham) was used to detect the secondary antibody as previously described (Thummel et al., 2008b; Vihtelic et al., 1999).

Constant intense-light treatment

Rod and cone photoreceptors were damaged in *albino* zebrafish using constant intense-light treatment (Vihtelic and Hyde, 2000; Vihtelic et al., 2006). Fish were dark adapted for 14 days and then were placed in tanks between four 250W halogen bulbs, which generated a light intensity of 6,000 lux. This constant intense light was maintained for up to 4 days, after which the fish were returned to standard light conditions (250 lux, 14 hours light: 10 hours dark).

Injection and electroporation of morpholinos in adult zebrafish retinas

Morpholino injection and electroporation was performed as previously described immediately prior to light treatment (Thummel et al., 2008b). Briefly, dark-adapted adult *albino* zebrafish were anesthetized, the outer most component of the cornea was removed with small forceps, a small incision was made in the cornea, and 0.5 μl of a 3 mM morpholino solution was injected into the vitreous of the left eye using a Hamilton syringe. The 3 mM cocktail that contained both *anti-pax6a* and *anti-pax6b* morpholinos had a final concentration of 1.5 mM of each morpholino. Immediately following the injections, the left eye was electroporated with a CUY21 Square Wave Electroporator (Protech International, Inc., San Antonio, TX), using 2 consecutive 50-msec pulses at 75 V with a 1 sec pause between pulses. A 3 mm diameter platinum plate electrode (CUY 650-P3 Tweezers, Protech International, Inc.) was used to drive the morpholino into the central and dorsal regions of the retina.

Bromodeoxyuridine labeling *in vivo*

Dark-adapted adult *albino* zebrafish were either uninjected or injected and electroporated with a 5-base mismatch control morpholino, *anti-pax6a* morpholino, or *anti-pax6b* morpholino as described above. After 24 hours of light treatment, fish were placed in a tank containing system water and 5 mM bromodeoxyuridine (BrdU) for 48 hours, as previously described (Bernardos et al., 2007).

Immunohistochemistry

Fish were euthanized at various time points during and following the constant light treatment by anesthetic overdose in 2-phenoxyethanol and eyes were collected. Unless otherwise noted, eyes were fixed in 9:1 ethanolic formaldehyde (100% ethanol:37% formaldehyde). After incubating overnight in fixative at 4°C, eyes were washed in 5% sucrose/1X PBS and cryoprotected in 30% sucrose/1X PBS overnight at 4°C. Eyes were subsequently washed in 1:1 Tissue Freezing Medium (TFM, Triangle Biomedical Sciences, Durham, NC):30% sucrose/1X PBS at 4°C overnight. The retinas were embedded in TFM and cryosectioned at a thickness of 14 microns. Frozen sections were dried at 50°C for two hours and subsequently stored at −80°C.

Prior to immunolabeling, slides were thawed for 20 minutes at 50°C and then rehydrated in 1X PBS. Retinal sections were incubated in blocking solution 1X PBS/2% NGS (normal goat serum)/0.2% Triton X-100/1% DMSO for 1 hour at room temperature prior to incubating overnight at 4°C with the primary antibody diluted in blocking buffer. Primary antibodies used for these studies include the mouse anti-PCNA monoclonal antibody (1:1000, clone PC10, Sigma Chemical, St. Louis, MO), rabbit anti-PCNA polyclonal antiserum (1:1500, Abcam, Cambridge, MA), rat anti-BrdU polyclonal antiserum (1:200, Accurate Chemical, Westbury, NY) rabbit anti-rhodopsin polyclonal antiserum (1:5000, (Vihtelic et al., 1999)), rabbit anti-UV opsin polyclonal antiserum (1:1000, (Vihtelic et al., 1999)), rabbit anti-blue opsin polyclonal antiserum (1:250, (Vihtelic et al., 1999)), rabbit anti-Pax6 polyclonal antiserum (1:100, Covance), rabbit anti-GFP polyclonal antiserum (1:

500, Abcam), and mouse anti-glutamine synthetase monoclonal antibody (1:500, Chemicon International, Temecula, CA). A modified antigen retrieval protocol was utilized for Pax6 immunostaining as previously described (Thummel et al., 2008a). Following incubation in primary antibody solution, sections were washed in 1X PBS/0.05% Tween-20 and then incubated for one hour at room temperature with the secondary antibody diluted 1:500 in 1X PBS/0.05% Tween-20. Secondary antibodies included Alexa Fluor goat anti-primary IgG 488, 568, 594, and 647 (Molecular Probes, Eugene, OR). Nuclei were labeled with TO-PRO-3 (Molecular Probes) at a 1:750 dilution in 1X PBS/0.05% Tween-20. Sections were washed again in 1X PBS/0.05% Tween-20 and 1X PBS before mounting with glass coverslips and ProLong Gold (Molecular Probes).

For BrdU immunolabeling, eyes were fixed in a 4% paraformaldehyde solution containing 5% sucrose/1X PBS, and embedded and sectioned as described above. Following rehydration, sections were washed in 1X PBS/0.3% Triton X-100 for 5 minutes, washed two times (5 minutes each) in DNaseI buffer (4.2 mM $MgCl_2$/150 mM NaCl/0.3% Triton X-100/0.5% DMSO), and then treated with 50 Kunitz/mL DNaseI (diluted in DNaseI buffer) for 10 minutes at room temperature. Sections were then washed twice in 1X PBS/ 0.3% Triton X-100 for 5 minutes at room temperature. Sections were blocked, incubated with anti-BrdU primary antiserum, washed and incubated with secondary antibody as described above.

For BrdU and PCNA colabeling, the BrdU protocol was followed and then sections were placed in 10 mM sodium citrate (pH 6.0) at 95° C for 20 minutes. Sections were left to cool for 20 minutes, washed twice in 1X PBS/0.3% Triton X-100 for 5 minutes, and then blocked as described above. BrdU and PCNA immunolocalizations were then performed as described above.

For TUNEL and PCNA colabeling, dark-adapted adult *albino* zebrafish were either uninjected or injected and electroporated with a 5-base mismatch control morpholino, anti-*pax6a* morpholino, or anti-*pax6b* morpholino. After 72 hours of constant light treatment, eyes were fixed, infiltrated and sectioned as described above. Following a wash in 1X PBS, the tissue was permeablized with a 5 minute wash in ice cold 1X PBS/ 0.1% NaCitrate/ 0.1% TritonX-100, followed by a wash in room temperature 1X PBS. TdT labeling (Clontech; Mountain View, CA) was performed per manufacturer's instructions, with one exception: biotin-conjugated dNTPs (New England Biolabs; Ipswich, MA) were used in place of the FITC-conjugated dNTPs. The labeling reaction was stopped by adding 2X SSC and the tissue was washed twice in 1X PBS. Blocking and primary antibody incubation were performed as described above. A fluorescent StrepAvidin-conjugate (1:200, Molecular Probes) was added with the secondary antibody mix (described above) and the slides were place in the dark for 1 hour at room temperature, washed in 1X PBS, and mounted with glass coverslips.

Statistical analysis of confocal microscopy

Confocal microscopy was performed with either a 1024 BioRad or Leica TCS SP5 confocal microscope. To maintain consistency between eyes and experimental groups, only retinal sections that contained or were immediately adjacent to the optic nerve were utilized. Quantification of individual cell types or nuclei was obtained from a linear distance of 740 microns in the central dorsal retina, which excluded the margin and optic nerve and corresponded to approximately half the linear distance of the dorsal retina. All quantification data is presented in Table 1. As clearly noted in the text and Table 1, between 6 and 15 retinas were analyzed per experiment, which is a standard sample size for adult zebrafish studies.

In each experiment, all data sets were first analyzed with a repeated measures ANOVA to first assess whether there were any significant differences between the various groups. The p-value for each of these tests were reported in Table 1. In experiments where the ANOVA revealed a statistically significant difference ($p<0.001$), two-sample t-tests were performed on each pair of samples and Bonferroni-corrected to account for the number of multiple tests. The individual significance levels (p-values) are reported in the body of the text.

RESULTS

Pax6a and Pax6b expression is efficiently reduced by electroporated morpholinos

As we previously reported, Pax6 was constitutively expressed in the amacrine cells in the INL and ganglion cells in the GCL in the undamaged adult zebrafish retina (Fig. 1A; (Thummel et al., 2008a)). Constant intense light treatment of dark-adapted *albino* zebrafish resulted in photoreceptor cell death and increased proliferation of rod precursor cells in the ONL at 16 hours (Fig. 1B), followed by Müller glia proliferation at 36 hours (Fig. 1C). Pax6 expression began colabeling with the proliferative marker PCNA in columns of neuronal progenitors after 36 hours of constant light and persisted through 96 hours (Fig. 1D, E), as they proliferated and migrated towards the ONL. Pax6 expression in the neuronal progenitors was largely absent by 3 days post light treatment (Thummel et al., 2008a), when the neuronal progenitors had finished migrating to the ONL and were differentiating into rods and cones. This temporal and spatial expression pattern of Pax6 corresponded to when neuronal progenitor cell proliferation and migration would be regulated.

We confirmed the efficiency and specificity of two previously published anti-*pax6* morpholino sequences to knockdown Pax6a and Pax6b protein expression (Blader et al., 2004) by microinjecting the morpholinos into 1–4 cell stage embryos (see Methods). Subsequent immunoblot analysis showed that each anti-*pax6* morpholino knocked down the desired Pax6 protein (Fig. 2).

We injected and electroporated either the anti-*pax6* or 5-base mismatch control (5mis) morpholinos into dark-adapted *albino* zebrafish retinas immediately before beginning the constant intense light treatment. After 72 hours in constant light, retinas were immunolabeled for Pax6 expression. Uninjected control retinas (Fig. 1F) exhibited Pax6 expression in the ganglion cells, amacrine cells, and neuronal progenitor cell clusters (Fig. 1F). Retinas injected and electroporated with either the 5mis MO-1 or 5mis MO-2 morpholinos were indistinguishable from the uninjected control, except for slightly elevated Pax6 expression in the inner plexiform layer (Fig. 1G, H). The *pax6a* morphant and *pax6a/pax6b* double morphant both possessed significantly reduced Pax6 expression in the ganglion cells, amacrine cells, and neuronal progenitor cell clusters relative to the controls (Fig. 1I, K). In contrast, the *pax6b* morphant exhibited normal Pax6 expression in the ganglion and amacrine cells, but reduced expression in the neuronal progenitor cell clusters relative to the controls (Fig. 1J). Thus, the ganglion and amacrine cells primarily expressed the Pax6a paralog, while the neuronal progenitors appeared to express both paralogs.

Pax6a and Pax6b are required at different points during neuronal progenitor proliferation

To examine if knockdown of either Pax6a or Pax6b expression affected cell proliferation in the regenerating retina, dark-adapted *albino* zebrafish were injected and electroporated with experimental and control morpholinos and then placed in constant light. After 36 hours of constant light, retinas in all groups exhibited PCNA-positive rod precursor cells and Müller glia (Supplementary Fig. 1A–D). Thus, neither Pax6 protein appeared to be required for either Müller glial or rod precursor cell division.

To examine if Pax6 was necessary for neuronal progenitor cell division, we examined the morphant retinas after 72 hours of constant light. The control retinas each possessed clusters of PCNA-positive neuronal progenitor cells associated with Müller glial cell processes (Fig. 3A–C). The *pax6a* morphant retina also exhibited clusters of PCNA-positive neuronal progenitors (Fig.3D), however, there was an average of only 3.8 ± 0.1 PCNA-positive progenitors in each *pax6a* morphant retinal cluster relative to 7.9 ± 0.7 PCNA-positive progenitors in each control cluster (Table 1; compared to uninjected control, p=0.003). Both the *pax6b* morphant and *pax6a/pax6b* double morphant contained an average of only 2 PCNA-positive neuronal progenitors per cluster (Fig. 3E, F; Table 1; compared to uninjected control, p=0.0005 and p=0.0007, respectively). Thus, knockdown of Pax6b expression inhibited the subsequent division of the Müller glia-derived INL neuronal progenitor. In contrast, reduction of Pax6a expression allowed this initial neuronal progenitor cell division, but it prevented later cell divisions.

To independently confirm the PCNA immunolabeling, we labeled proliferating progenitors with BrdU between 24 and 72 hours of light treatment. As expected, BrdU colabeled with PCNA in the dividing neuronal progenitors after 72 hours of constant light treatment (Fig. 4A). Furthermore, the BrdU-labeled neuronal progenitors were associated with GFAP-positive Müller glial processes (Fig. 4B). Three days after completing the four days of constant intense light treatment, large numbers of INL neuronal progenitor cells had migrated to the ONL (Raymond et al., 2006) and were observed to be BrdU-positive (Fig. 4C). In addition, the Müller glial cell nuclei that initially divided around 36 hours of constant light treatment remained BrdU-positive (Fig. 4C).

After 72 hours of constant light treatment, control retinas incorporated BrdU in clusters of neuronal progenitors that each contained an average of 7.4 to 8.1 nuclei (Fig. 4D–F; Table 1). In contrast, the *pax6a* morphant retinas (Fig. 4G) contained an average of only 4.6 BrdU-labeled nuclei per cluster (Table 1; compared to uninjected control, p=0.01). Further, the *pax6b* morphant and *pax6a/pax6b* double morphant retinas possessed an average of only 2.3 and 2.0 BrdU-labeled nuclei per cluster, respectively (Fig. 4H, I; Table 1, compared to uninjected control, p=0.001 and p=0.0008, respectively). These data suggest that the asymmetric Müller glial cell division to produce the first neuronal progenitor does not require Pax6 expression, while the subsequent division of the neuronal progenitor cell needs Pax6b expression. Furthermore, Pax6a was only required for one of the final rounds of progenitor cell division in each cluster.

Reduced numbers of neuronal progenitors observed in *pax6* morphants is not a result of increased cell death

We previously reported that knockdown of PCNA during constant intense light treatment inhibited Müller glial cell division (Thummel et al., 2008b). Because Müller glial cell division cannot occur without necessary levels of PCNA, these activated Müller glia died, with TUNEL-positive Müller glia observed 12 hours following the failed division (Thummel et al., 2008b). Given that we observed reduced numbers of dividing neuronal progenitors in *pax6a* and *pax6b* morphant retinas, it is possible that Pax6 is required for neuronal progenitor cell survival. We took two approaches to determine whether this was the case. First, control and morphant retinas were analyzed for the presence of TUNEL-positive nuclei at 72 hours of constant light treatment. Based on our previous findings, if neuronal progenitors were dying as a result of Pax6 knockdown, then TUNEL-positive nuclei would be present in the INL at this time point. Similar to a previous report (Bernardos 2007), very few TUNEL-positive nuclei were observed in the ONL of either the control or morphant retinas (Fig 5). Importantly, no TUNEL-positive nuclei were visualized in the INL of the controls, *pax6a* or *pax6b* morphant retinas (Fig. 5). Colabeling with PCNA confirmed that neuronal progenitors were present in these retinas, but were not TUNEL-positive (Fig. 5).

Second, we analyzed control and morphant retinas after 4 days of constant intense light followed by recovery in 3 days of standard light. We found the PCNA-positive INL nuclei persisted in both the *pax6b* and *pax6a/pax6b* morphants (Fig. 6K, L), indicating that these cells have not died, but were still present many days after their initial entrance into the cell cycle. Together, these data show that neuronal progenitors are not dying as a result of either Pax6a or Pax6b knockdown.

Rod precursor proliferation is inversely proportional to the number of INL neuronal progenitors

To examine the subsequent effects of Pax6 knockdown, we injected and electroporated the morpholinos into dark-adapted *albino* zebrafish retinas and analyzed the retinas after 4 days of constant intense light followed by recovery in 3 days of standard light. The control retinas possessed newly regenerated rhodopsin-positive rod photoreceptors (Fig. 6A–C), with PCNA expression primarily restricted to the ONL rod precursor cells (Fig. 6G–I). The *pax6a* morphant retina exhibited reduced rhodopsin expression relative to the control retinas (Fig. 6D), suggesting that fewer rods had regenerated in the *pax6a* morphant compared to the control retinas. Strikingly, both the *pax6b* morphant and *pax6a/pax6b* double morphant retinas possessed only isolated and short rhodopsin-positive rod outer segments (Fig. 6E, F), suggesting that even fewer rods had regenerated relative to the *pax6a* morphant.

We also quantified the number of PCNA-positive nuclei at this timepoint. As noted above, the *pax6b* morphant and *pax6a/pax6b* double morphant retinas still possessed the doublets of PCNA-positive INL cells (Fig. 6K, L), which were first observed at 72 hours of constant light (Fig. 3 and Fig. 4). Thus, in the absence of Pax6b, INL neuronal progenitors failed to migrate to the ONL. However, surprisingly, the *pax6b* morphant and *pax6a/pax6b* double morphant retinas contained over twice the number of PCNA-positive ONL cells relative to the controls (Table 1; compared to uninjected control, p=0.0008 and p=0.001, respectively). Given the apparent lack of neuronal progenitor cell migration from the INL in these morphant retinas, the large number of proliferating ONL cells represented resident ONL rod precursors. Therefore, these data suggested that the number of INL neuronal progenitors that migrated to the ONL proportionally reduced the number of proliferating ONL rod precursor cells. Data from the *pax6a* morphants further supported this hypothesis. Similar to the control retinas, the *pax6a* morphant retinas contained very few PCNA-positive neuronal progenitors in the INL at this time point (Fig. 6G–J), suggesting that the few neuronal progenitors observed in the *pax6a* morphant retinas did migrate to the ONL. In addition, the *pax6a* morphant retina contained an intermediate number of PCNA-positive ONL nuclei (118.4 ± 20.3), which was greater than the control retinas (70.5 to 78.4, Table 1; p=0.04), but fewer than observed in the *pax6b* retinas (161 ± 11.4, Table 1). Together, these data suggest that rod precursor proliferation is inversely proportional to the number of INL neuronal progenitors that migrate to the ONL during photoreceptor regeneration.

Pax6-stimulated neuronal progenitors are required for cone cell regeneration

The failure of neuronal progenitors to migrate to the ONL in the *pax6b* morphant and *pax6a/pax6b* double morphant retinas allowed us to determine if they were required to regenerate a specific class of photoreceptor. At 28 days following the completion of the constant light treatment, the control and experimental retinas all exhibited robust rhodopsin localization (Fig. 7A–E) and an equivalent number of rod photoreceptor nuclei in the ONL (Table 1). In contrast, significantly fewer long and short single cones were present in the *pax6b* morphant and *pax6a/pax6b* double morphant retinas relative to the controls (Fig. 7I, J, N and O; Table 1; compared to uninjected control, p=0.002 and p=0.002 for long single cones, respectively). Furthermore, the *pax6a* morphant retina exhibited a level of cone cell regeneration intermediate to the controls and the *pax6b* morphant and *pax6a/pax6b* double morphants

(Fig. 7H, M; Table 1; compared to uninjected control, p=0.04 for long single cones), although this value was not statistically significant relative to the controls. This level of cone cell regeneration corresponded to the relative number of neuronal progenitors present in each INL cluster (Fig. 3 and Fig. 4; Table 1). This suggested that Pax6-dependent INL neuronal progenitor proliferation was necessary for regeneration of cones and not rods, while the ONL rod precursors were sufficient for regeneration of rods.

DISCUSSION

Unlike the mammalian retina, the adult zebrafish possess the ability to specifically regenerate all retinal cell types (Bernardos et al., 2007; Fausett and Goldman, 2006; Fimbel et al., 2007; Raymond et al., 2006; Vihtelic and Hyde, 2000; Wolburg, 1975; Yurco and Cameron, 2005). Zebrafish retinal regeneration originates from two stem cell populations: the INL Müller glia and the ONL rod precursors (Bernardos et al., 2007; Fausett and Goldman, 2006; Morris et al., 2008b; Morris et al., 2005; Thummel et al., 2008b; Yurco and Cameron, 2005). Müller glia reenter the cell cycle and produce multipotent neuronal progenitors, which continue to divide and migrate to the damaged nuclear layer, where they differentiate into the neuronal cell types that were lost. Rod precursors can also reenter the cell cycle when rod photoreceptors are lost and differentiate into only rods (*data not shown*, Fig. 3 and Fig. 4). In the case of chronic rod cell death (Morris et al., 2005), however, only rod precursor proliferation is observed.

This study builds on the observed increase in *pax6b* mRNA expression and the increased Pax6 protein expression during regeneration of the light-damaged retina (Raymond et al., 2006; Thummel et al., 2008a). We also previously demonstrated that the *pax6b* mRNA expression increased first, immediately following Müller glial cell division, followed by increased *pax6a* mRNA expression when neuronal progenitors were undergoing rapid cell divisions (Thummel et al., 2008a). Using morpholinos that were electroporated into the retina to knockdown the expression of either one or both of the Pax6 proteins, we examined the functions of Pax6a and Pax6b during regeneration of rods and cones. Knockdown of Pax6a, Pax6b, or both proteins had no effect on the ability of Müller glia or rod precursors to enter the cell cycle (Supplementary Fig. 3). Because we never observed Pax6 expression in rod precursors, this was not surprising. However, it was reported that very weak Pax6 expression was detected in the Müller glia of undamaged retinas (Bernardos et al., 2007). Although we failed to detect Pax6 expression in the Müller glia prior to retinal damage (Fig. 1A), our functional data clearly demonstrated that neither Pax6 paralog was required for the initiation of Müller glial cell division. Furthermore, these data showed that the previously-published morpholinos used in this study did not cause any non-specific delays in the regenerative timecourse (Blader et al., 2004).

The adult zebrafish regeneration response initiates with the Müller glia reentering the cell cycle (Fig. 8). This could be either an asymmetric cell division to yield a Müller glial cell and a neuronal progenitor cell or the Müller glial cell may dedifferentiate and then divide to yield two neuronal progenitor cells. Regardless of the mechanism underlying this first cell division, the second cell division requires the Pax6b protein. In contrast, knockdown of the Pax6a protein does not disrupt this second cell division, which may be because the *pax6a* gene is not expressed at this point in regeneration. This temporal sequence is consistent with the expression of *pax6b* increasing prior to *pax6a* during regeneration of the light-damaged retina, as we previously reported (Thummel et al., 2008a). Alternatively, it is possible that Pax6b is a stronger regulator of neuronal progenitor proliferation, as has been previously suggested (Nornes et al., 1998). Thus, we cannot differentiate if the Pax6b protein regulates a different set of genes than Pax6a, which separates the functions of these two proteins at this second cell division, or if the two proteins regulate the same set of target genes and that

they differ simply in their temporal expression and/or strength of activation. Furthermore, it is unclear if photoreceptor cell regeneration requires Pax6 expression in the neuronal progenitor cells or in the amacrine and ganglion cells. While it seems most likely that Pax6 expression in these neuronal progenitor cells would be required to regulate their proliferation, it is possible that Pax6 expression in the adjacent amacrine and ganglion cells may be necessary to regulate neuronal progenitor cell proliferation through a secreted factor. Definitive proof of either of these two models will require the knockdown of Pax6 expression in specific cell types.

The neuronal progenitors continue to divide, if Pax6b is present, until they reach 4 cells in each INL cluster (Fig. 8). At this point, the Pax6a protein is required to activate the expression of specific target genes to allow the continued proliferation of the progenitors. However, in the absence of Pax6a, the four progenitors will migrate to the ONL sometime between 3 and 7 days of starting the constant light treatment. In contrast, the two progenitor cell clusters in the *pax6b* morphant are still present 7 days after starting the constant light treatment. The persistence of these progenitors and the absence of TUNEL-positive nuclei in the INL (Fig. 5) clearly show that neuronal progenitors are not dying as a result of Pax6b knockdown. However, it is unclear what mechanism allows for the migration of the four neuronal progenitors in the *pax6a* morphant retinas, but does not allow for the migration of the two neuronal progenitors in the *pax6b* and *pax6a/pax6b* morphant retinas. Because BrdU would incorporate into both the INL and ONL progenitors at all time points, a standard cell tracking study would not differentiate the origin of the ONL progenitors. Thus, we cannot differentiate between Müller glial-derived rod photoreceptors and rod precursor-derived rod photoreceptors during the regeneration response. However, the development of new genetic technologies, transgenic zebrafish lines, and antisera that are specific to the individual cell lineages may allow for future resolution of this question (Bernardos and Raymond, 2006;Hitchcock and Kakuk-Atkins, 2004;Kassen et al., 2007;Morris et al., 2008b).

The failure of the neuronal progenitors to migrate to the ONL in the *pax6b* morphant and *pax6a/pax6b* double morphant resulted in twice the number of proliferating ONL rod precursors as the control retinas (Table 1). In contrast, the *pax6a* morphant retina produced clusters consisting of four proliferating neuronal progenitor cells that appeared to migrate to the ONL, which was approximately half the number as the control retinas. This resulted in an intermediate number of proliferating ONL rod precursors relative to the control and the *pax6b* morphant retinas. Taken together, the proliferation of the resident rod precursor cells in the ONL, which are committed to becoming rods, may be negatively regulated by the relative number of INL neuronal progenitors that migrate to the ONL during regeneration of the light-damaged retina. This model implies that the migrating neuronal progenitors from the INL repress the proliferation of the resident ONL rod precursor cells. Furthermore, the increased number of PCNA-positive rod precursor cells in both the *pax6b* and the *pax6a* morphant retinas clearly shows that rod precursor proliferation is not directly dependent of Pax6. It is likely that many of the increased number of proliferating ONL rod precursors in the *pax6b* and *pax6a* morphant retinas, relative to the control retinas, ultimately die because all the retinas contain nearly equivalent numbers of regenerated rods. However, we were unable to detect the death of these proliferating rod precursor cells in the *pax6a* and *pax6b* morphant retinas, likely due to our inability to identify the proper time point when this cell death was occurring.

The control and *pax6* morphant retinas all exhibited an equivalent number of regenerated rods. The apparent failure of the *pax6b* morphant and *pax6a/pax6b* double morphant retinas to generate neuronal progenitors that migrated to the ONL indicates that the regenerated rods in these morphants were derived entirely from rod precursors. The regeneration of rods from resident ONL rod precursors in the light-damaged *pax6b* morphant retina is consistent

with the persistent proliferation and attempted regeneration of rods in the chromic rod-less transgenic line Tg(*XOPS::mCFP*)^{QO1} (Morris et al., 2008b; Morris et al., 2005). Furthermore, examination of the number of regenerated cones in the control and *pax6* morphant retinas was proportional to the number of neuronal progenitors that migrated to the ONL. Thus, this is the first report to demonstrate that the regeneration of cones requires proliferation of the Müller glial-derived neuronal progenitor cells, while rods can be regenerated from increased amplification of resident ONL rod precursors.

In addition to adding to the growing number of works that seek to characterize the molecular requirements of Müller glia-derived neuronal regeneration, our results detail three novel findings. First, Pax6a and Pax6b are the first transcription factors shown to specifically and differentially regulate neuronal progenitor cell proliferation during regeneration of the adult vertebrate retina. This is in stark contrast to the requirement of Ascl1a and Stat3 for the initial proliferation of the Müller glia in the damaged zebrafish retina (Fausett et al., 2008; Kassen et al., 2010). Thus, Pax6a and Pax6b define steps subsequent to Ascl1a and Stat3 in retinal regeneration. Second, our results demonstrate an inverse relationship between the number of Müller glial-derived INL neuronal progenitors migrating to the ONL and the extent of proliferation of the resident ONL rod precursors. This communication between the migrating INL neuronal progenitors and the resident ONL rod precursors defines a previously unrecognized event in regulating the regeneration response in the adult zebrafish retina. Finally, these data strongly suggest distinct mechanisms are required for selective rod and cone photoreceptor regeneration.

Supplementary Material

Refer to Web version on PubMed Central for supplementary material.

Acknowledgments

We thank D. Bang and the staff of the Freimann Life Science Center for providing zebrafish husbandry and care. This work was funded by National Institutes of Health grants R21EY018919 (D.R.H.) and R01EY018417 (D.R.H. and R.T.), the Center for Zebrafish Research at the University of Notre Dame, and a Fight for Sight Postdoctoral Research fellowship (R.T.).

REFERENCES

Bernardos RL, Barthel LK, Meyers JR, Raymond PA. Late-stage neuronal progenitors in the retina are radial Muller glia that function as retinal stem cells. J Neurosci 2007;27:7028–7040. [PubMed: 17596452]

Bernardos RL, Raymond PA. GFAP transgenic zebrafish. Gene Expr Patterns 2006;6:1007–1013. [PubMed: 16765104]

Blader P, Lam CS, Rastegar S, Scardigli R, Nicod JC, Simplicio N, Plessy C, Fischer N, Schuurmans C, Guillemot F, Strahle U. Conserved and acquired features of neurogenin1 regulation. Development 2004;131:5627–5637. [PubMed: 15496438]

Braisted JE, Essman TF, Raymond PA. Selective regeneration of photoreceptors in goldfish retina. Development 1994;120:2409–2419. [PubMed: 7956821]

Bringmann A, Pannicke T, Grosche J, Francke M, Wiedemann P, Skatchkov SN, Osborne NN, Reichenbach A. Muller cells in the healthy and diseased retina. Prog Retin Eye Res 2006;25:397–424. [PubMed: 16839797]

Cameron DA. Cellular proliferation and neurogenesis in the injured retina of adult zebrafish. Vis Neurosci 2000;17:789–797. [PubMed: 11153658]

Detrich HW 3rd, Westerfield M, Zon LI. Overview of the Zebrafish system. Methods Cell Biol 1999;59:3–10. [PubMed: 9891351]

Fausett BV, Goldman D. A role for alpha1 tubulin-expressing Muller glia in regeneration of the injured zebrafish retina. J Neurosci 2006;26:6303–6313. [PubMed: 16763038]

Fausett BV, Gumerson JD, Goldman D. The proneural basic helix-loop-helix gene ascl1a is required for retina regeneration. J Neurosci 2008;28:1109–1117. [PubMed: 18234889]

Fimbel SM, Montgomery JE, Burket CT, Hyde DR. Regeneration of inner retinal neurons after intravitreal injection of ouabain in zebrafish. J Neurosci 2007;27:1712–1724. [PubMed: 17301179]

Hitchcock P, Kakuk-Atkins L. The basic helix-loop-helix transcription factor neuroD is expressed in the rod lineage of the teleost retina. J Comp Neurol 2004;477:108–117. [PubMed: 15281083]

Hitchcock PF, Lindsey Myhr KJ, Easter SS Jr, Mangione-Smith R, Jones DD. Local regeneration in the retina of the goldfish. J Neurobiol 1992;23:187–203. [PubMed: 1527527]

Hitchcock PF, Raymond PA. The teleost retina as a model for developmental and regeneration biology. Zebrafish 2004;1:257–271. [PubMed: 18248236]

Kassen SC, Ramanan V, Montgomery JE, C TB, Liu CG, Vihtelic TS, Hyde DR. Time course analysis of gene expression during light-induced photoreceptor cell death and regeneration in albino zebrafish. Dev Neurobiol 2007;67:1009–1031. [PubMed: 17565703]

Kassen SC, Raycroft FJ, Thummel R, Plasschaert R, Hyde DR. Stat3 is required for maximal Müller glial cell proliferation during regeneration of the light-damaged zebrafish retina. J Neurosci. 2010 October; Under Review, 2009.

Lawrence JM, Singhal S, Bhatia B, Keegan DJ, Reh TA, Luthert PJ, Khaw PT, Limb GA. MIO-M1 cells and similar muller glial cell lines derived from adult human retina exhibit neural stem cell characteristics. Stem Cells 2007;25:2033–2043. [PubMed: 17525239]

Maier W, Wolburg H. Regeneration of the goldfish retina after exposure to different doses of ouabain. Cell Tissue Res 1979;202:99–118. [PubMed: 509506]

Marcus RC, Delaney CL, Easter SS Jr. Neurogenesis in the visual system of embryonic and adult zebrafish (Danio rerio). off. Vis Neurosci 1999;16:417–424. [PubMed: 10349963]

Morris AC, Scholz T, Fadool JM. Rod progenitor cells in the mature zebrafish retina. Adv Exp Med Biol 2008a;613:361–368. [PubMed: 18188965]

Morris AC, Scholz TL, Brockerhoff SE, Fadool JM. Genetic dissection reveals two separate pathways for rod and cone regeneration in the teleost retina. Dev Neurobiol 2008b;68:605–619. [PubMed: 18265406]

Morris AC, Schroeter EH, Bilotta J, Wong RO, Fadool JM. Cone survival despite rod degeneration in XOPS-mCFP transgenic zebrafish. Invest Ophthalmol Vis Sci 2005;46:4762–4771. [PubMed: 16303977]

Nornes S, Clarkson M, Mikkola I, Pedersen M, Bardsley A, Martinez JP, Krauss S, Johansen T. Zebrafish contains two pax6 genes involved in eye development. Mech Dev 1998;77:185–196. [PubMed: 9831649]

Otteson DC, D'Costa AR, Hitchcock PF. Putative stem cells and the lineage of rod photoreceptors in the mature retina of the goldfish. Dev Biol 2001;232:62–76. [PubMed: 11254348]

Otteson DC, Hitchcock PF. Stem cells in the teleost retina: persistent neurogenesis and injury-induced regeneration. Vision Res 2003;43:927–936. [PubMed: 12668062]

Raymond PA, Barthel LK, Bernardos RL, Perkowski JJ. Molecular characterization of retinal stem cells and their niches in adult zebrafish. BMC Dev Biol 2006;6:36. [PubMed: 16872490]

Rowan S, Cepko CL. Genetic analysis of the homeodomain transcription factor Chx10 in the retina using a novel multifunctional BAC transgenic mouse reporter. Dev Biol 2004;271:388–402. [PubMed: 15223342]

Stenkamp DL. Neurogenesis in the fish retina. Int Rev Cytol 2007;259:173–224. [PubMed: 17425942]

Thummel R, Kassen SC, Enright JM, Nelson CM, Montgomery JE, Hyde DR. Characterization of Muller glia and neuronal progenitors during adult zebrafish retinal regeneration. Exp Eye Res 2008a;87:433–444. [PubMed: 18718467]

Thummel R, Kassen SC, Montgomery JE, Enright JM, Hyde DR. Inhibition of Muller glial cell division blocks regeneration of the light-damaged zebrafish retina. Dev Neurobiol 2008b;68:392–408. [PubMed: 18161852]

Vihtelic TS, Doro CJ, Hyde DR. Cloning and characterization of six zebrafish photoreceptor opsin cDNAs and immunolocalization of their corresponding proteins. Vis Neurosci 1999;16:571–585. [PubMed: 10349976]

Vihtelic TS, Hyde DR. Light-induced rod and cone cell death and regeneration in the adult albino zebrafish (Danio rerio) retina. J Neurobiol 2000;44:289–307. [PubMed: 10942883]

Vihtelic TS, Soverly JE, Kassen SC, Hyde DR. Retinal regional differences in photoreceptor cell death and regeneration in light-lesioned albino zebrafish. Exp Eye Res 2006;82:558–575. [PubMed: 16199033]

Westerfield, M. The Zebrafish Book: A guide for the laboratory use of zebrafish (Danio rerio). Eugene, OR: Univ. of Oregon Press; 1995.

Wolburg H. Time- and dose-dependent influence of ouabain on the ultrastructure of optic neurones. Cell Tissue Res 1975;164:503–517. [PubMed: 1203964]

Wu DM, Schneiderman T, Burgett J, Gokhale P, Barthel L, Raymond PA. Cones regenerate from retinal stem cells sequestered in the inner nuclear layer of adult goldfish retina. Invest Ophthalmol Vis Sci 2001;42:2115–2124. [PubMed: 11481280]

Xu S, Sunderland ME, Coles BL, Kam A, Holowacz T, Ashery-Padan R, Marquardt T, McInnes RR, van der Kooy D. The proliferation and expansion of retinal stem cells require functional Pax6. Dev Biol 2007;304:713–721. [PubMed: 17316600]

Yurco P, Cameron DA. Responses of Muller glia to retinal injury in adult zebrafish. Vision Res 2005;45:991–1002. [PubMed: 15695184]

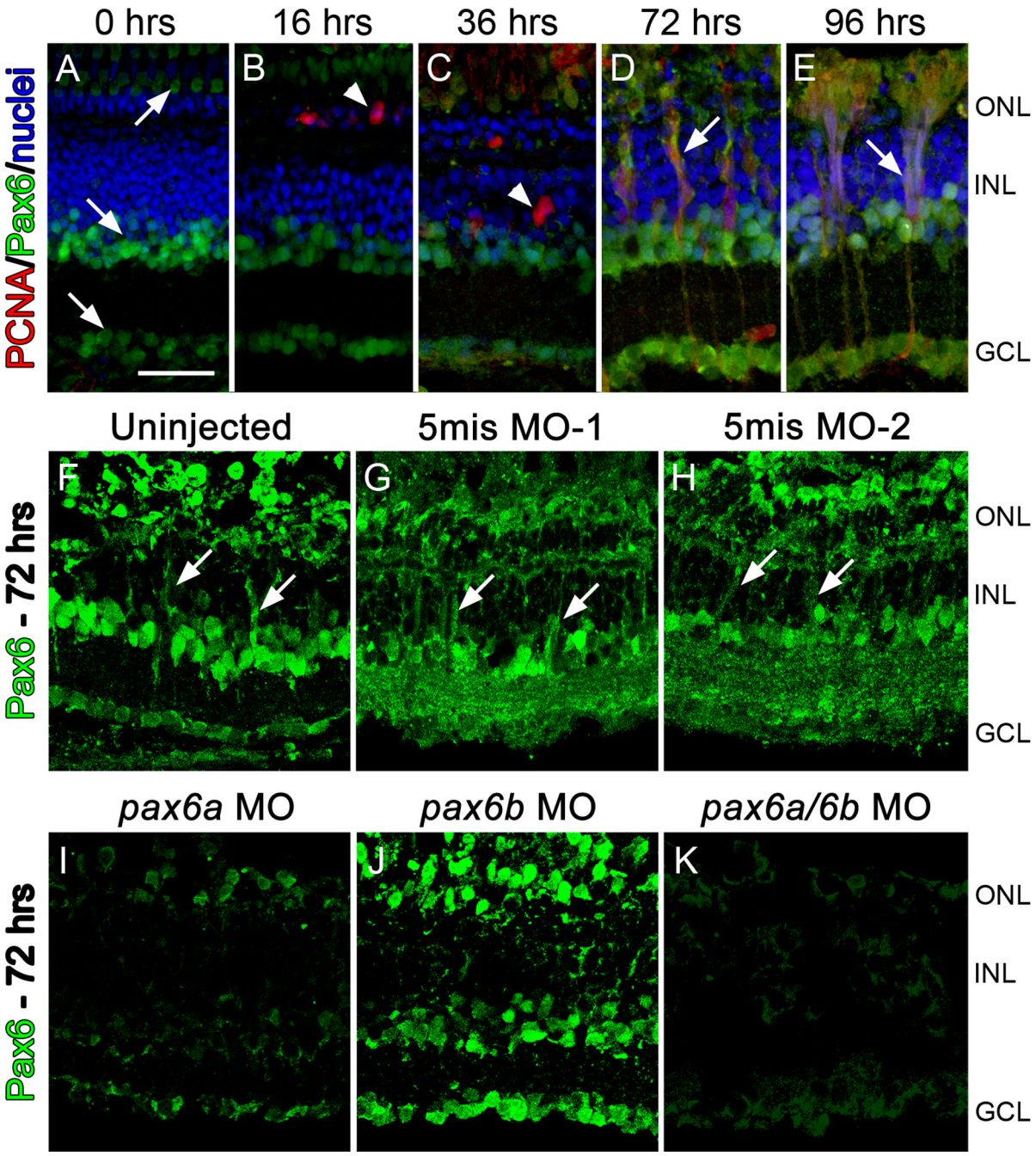

Figure 1. Knockdown of Pax6 in the regenerating zebrafish retina

Pax6 expression (green), PCNA expression (red), and nuclei (blue) were examined during intense light treatment. Throughout the timecourse, Pax6 expression was observed in mature amacrine cells (A, arrow in INL) and ganglion cells (A, arrow in GCL). Pax6 expression in the photoreceptor layer, particularly in the cones (A, arrow in ONL), likely represents non-specific binding of the primary antibody as it is highly variable, even on adjacent tissue sections. Pax6 expression did not colabel with proliferating rod precursors (B, 16 hrs, arrowhead) or with proliferating Müller glia (C, 36 hrs, arrowhead). Pax6 expression was observed in proliferating neuronal progenitors at 72 and 96 hrs (D and E, respectively, arrows). To test the efficacy and specificity of the anti-*pax6* morpholinos, zebrafish were

either uninjected or injected and electroporated with one of two 5-base mismatch control morpholinos, with anti-*pax6a* morpholino, anti-*pax6b* morpholino, or a cocktail of both morpholinos. Pax6 expression (green) was assessed after 72 hrs of constant light treatment (Panels F–K). The uninjected (F), 5mis MO-1 (G), and 5mis MO-2 retinas (H) all contained large columns of neuronal progenitor cells that colabeled with Pax6 (arrows). Knockdown of only the Pax6a paralog (I) or both Pax6a and Pax6b (Panel K) resulted in a loss of nearly all Pax6 expression. However, Pax6-positive amacrine and ganglion cells were detected in the *pax6b* morphant retina (J), although Pax6 expression in the columns of neuronal progenitors was reduced. The scale bar in panel A represents 25 microns and is the same for panels B–K. GCL, ganglion cell layer; INL, inner nuclear cell layer; ONL, outer nuclear layer.

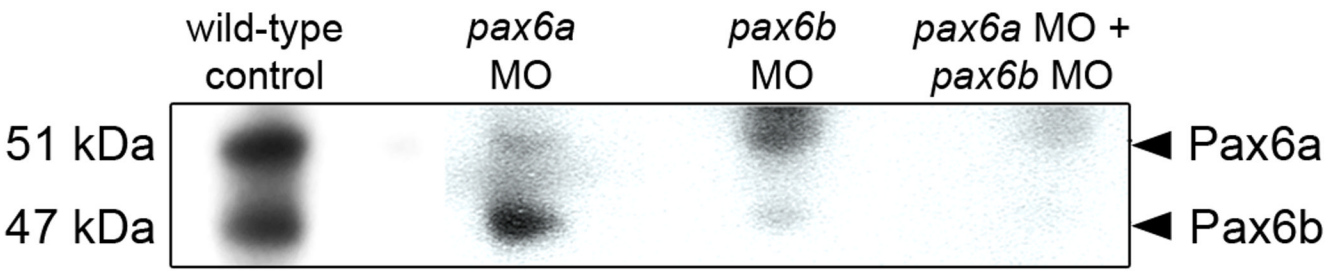

Figure 2. Efficient and specific morpholino-induced knockdown of Pax6a and Pax6b during embryonic development

Immunoblot analysis with the rabbit anti-Pax6 polyclonal antisera detected both Pax6a and Pax6b paralogs (51 and 47 kDa, respectively) in wild-type zebrafish embryos (lane 1). The anti-*pax6a* and anti-*pax6b* morpholinos (*pax6a* MO and *pax6b* MO, respectively) selectively knockdown the expression of the expected Pax6 paralogs (lanes 2 and 3, respectively). Coinjection of both morpholinos (*pax6a* MO + *pax6b* MO) significantly reduced the expression of both Pax6 proteins (lane 4).

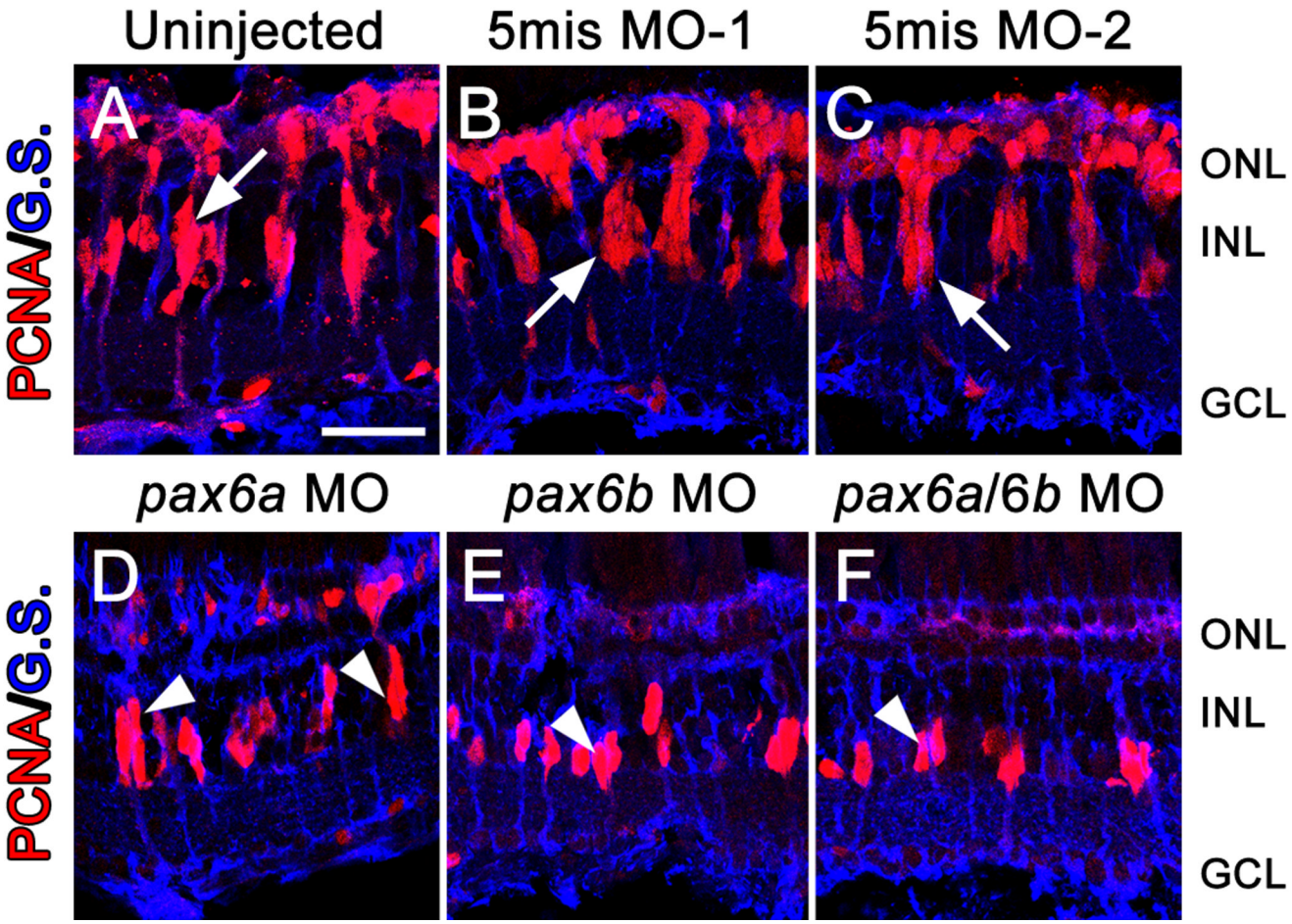

Figure 3. Pax6 is required for proliferation of Müller glial-derived neuronal progenitors

Dark-adapted adult *albino* zebrafish were either uninjected or injected and electroporated with one of two 5-base mismatch control morpholinos (5mis MO-1 and 5mis MO-2), anti-*pax6a* morpholino, anti-*pax6b* morpholino, or a cocktail of both morpholinos. PCNA (red) and Glutamine synthetase (blue) expression were assessed after 72 hrs of constant light treatment by immunohistochemistry. The uninjected and 5mis MO retinas (A–C) all contained large columns of PCNA-positive neuronal progenitor cells associated with Müller glial cell processes (arrow). However, knockdown of only the Pax6a paralog (D) yielded columns (arrowheads) that contained fewer PCNA-positive cells relative to controls. In contrast, knockdown of only Pax6b (E) or both Pax6a and Pax6b (F) produced clusters of neuronal progenitors (arrowheads) that were fewer in number than the *pax6a* morphant retina. The scale bar in panel A represents 25 microns and is the same for panels B–F. GCL, ganglion cell layer; INL, inner nuclear cell layer; ONL, outer nuclear layer.

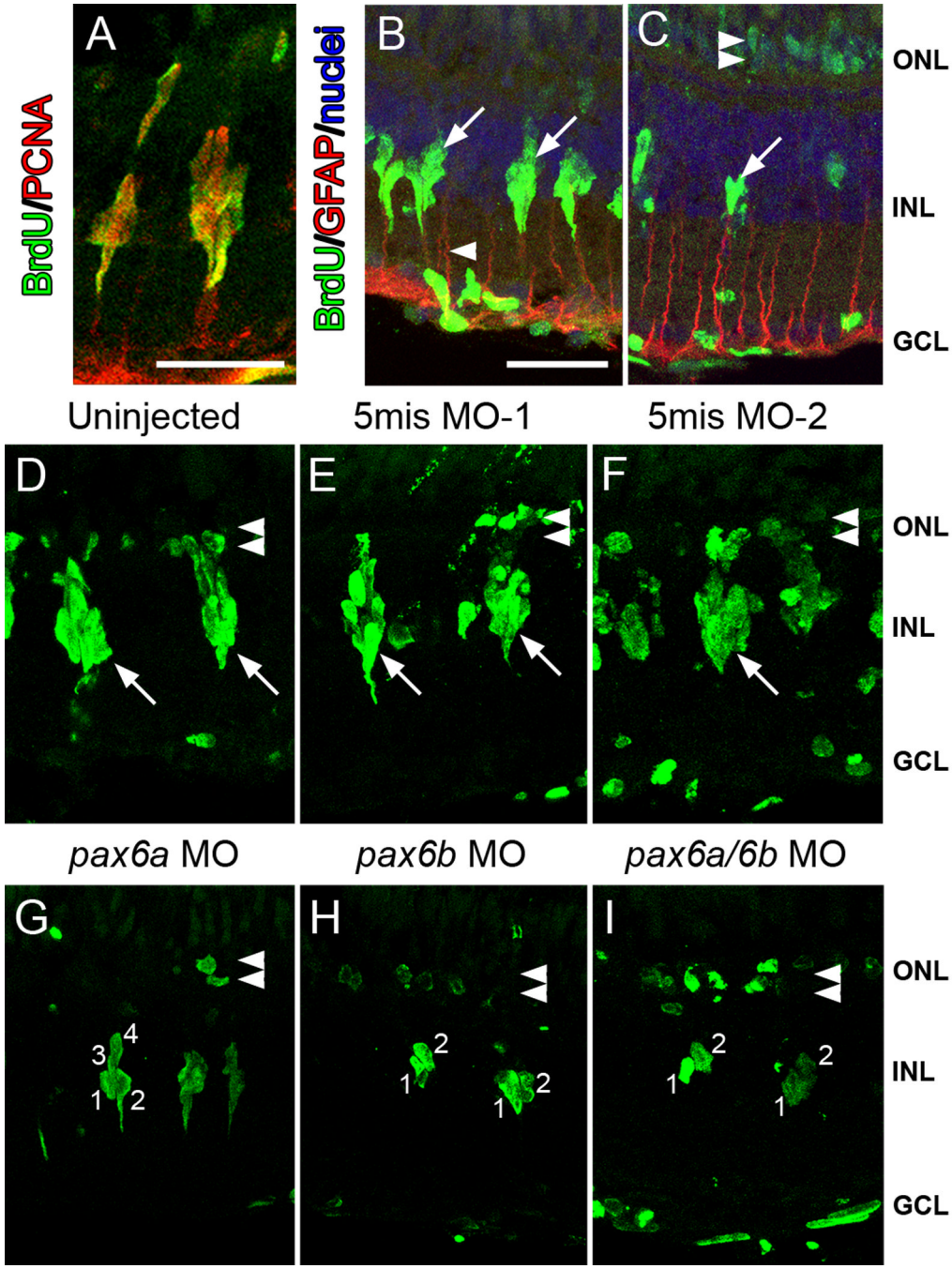

Figure 4. BrdU incorporation reveals that Pax6a and Pax6b both function at different stages of neuronal progenitor proliferation

In uninjected retinas, after 72 hours of light treatment, BrdU (green) colabeled with PCNA (red) in columns of proliferating neuronal progenitors in the INL (A), while BrdU-positive neuronal progenitors (green) were associated with GFAP-labeled (red) Müller glial processes (B, arrowhead). (C) Three days following completion of the light treatment, BrdU-positive nuclei (green) were visualized in the ONL (double arrowhead), corresponding to the daughter cells of the INL neuronal progenitors, and the individual Müller cells (arrows) that were the source of the neuronal progenitors. (D–I) After 72 hours of constant light, BrdU-labeled nuclei (green) were observed in the ONL of control and experimental

retinas (double arrowheads). Large clusters of BrdU-labeled neuronal progenitors were also observed in the INL (arrows) of uninjected (D), the 5mis MO-1 (E), and the 5mis MO-2 (F) retinas. In contrast, *pax6a* morphant retinas (G) contained an average of only four BrdU-positive nuclei per cluster. Strikingly, *pax6b* morphant and *pax6a/pax6b* double morphant retinas (H and I, respectively) possessed an average of only two BrdU-labeled nuclei per cluster, which was consistent with the Müller cell only dividing once and no proliferation of the neuronal progenitors. The scale bar in panel A represents 25 microns and is the same for panels D–I, while the scale bar in panel B represents 25 microns and is the same for panel C. GCL, ganglion cell layer; INL, inner nuclear cell layer; ONL, outer nuclear layer.

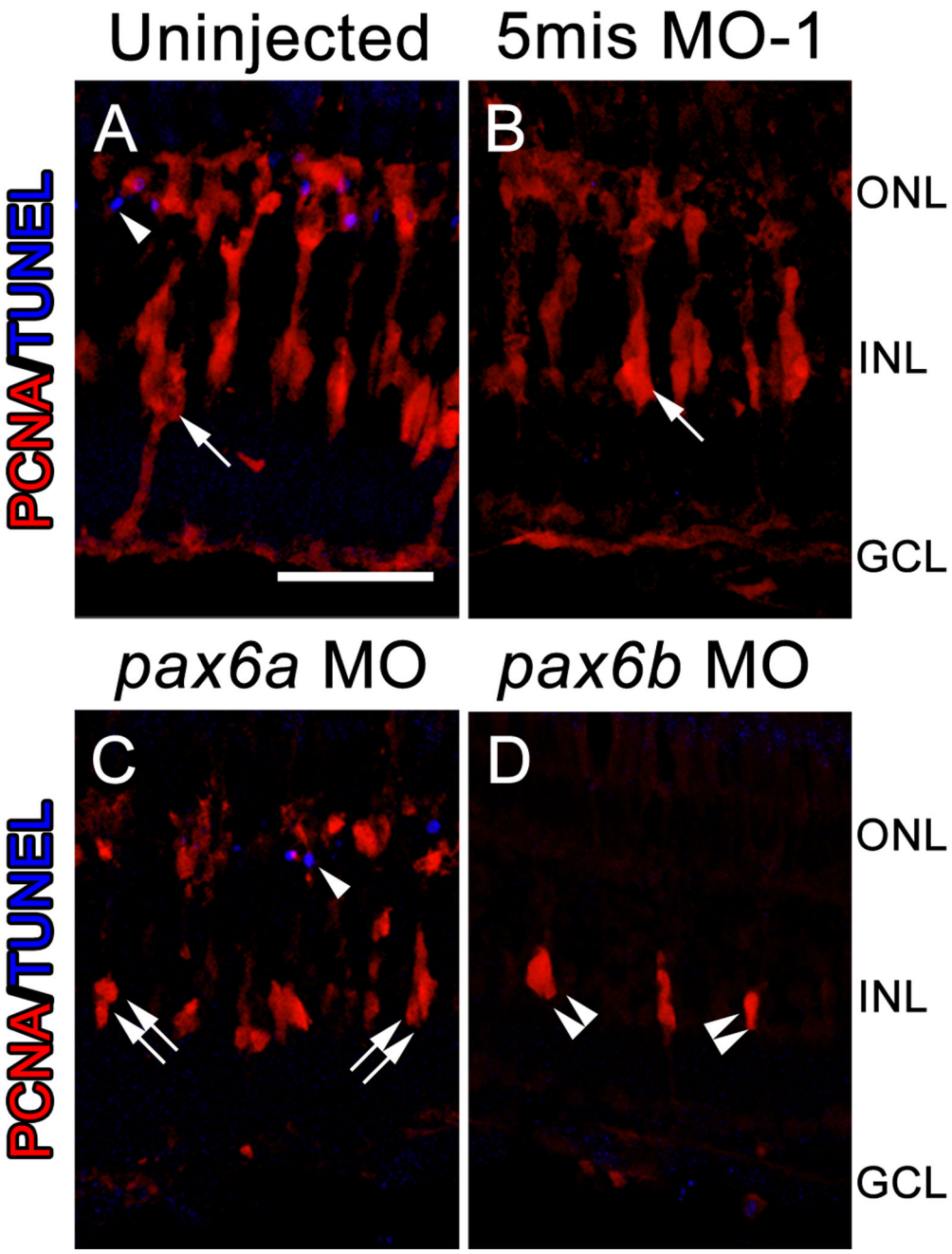

Figure 5. Reduced numbers of INL neuronal progenitors observed in the *pax6* morphants is not a result of increased cell death

Dark-adapted adult *albino* zebrafish were either uninjected or injected and electroporated with a 5-base mismatch control morpholino (5mis MO-1), anti-*pax6a* morpholino, or anti-*pax6b* morpholino. PCNA expression (red) and TUNEL labeling (blue) were assessed after 72 hours of constant light treatment by immunohistochemistry. The uninjected and 5mis MO-1 retinas (A, B) both contained large columns of PCNA-positive neuronal progenitor cells (arrow). However, knockdown of only Pax6a (C) yielded columns (double arrows) that contained fewer PCNA-positive cells relative to controls. In contrast, knockdown of only Pax6b (D) produced clusters of neuronal progenitors (double arrowheads) that were fewer in

number than even the *pax6a* morphant retina. TUNEL-positive nuclei (single arrowheads) were occasionally observed in the ONL of both the control and *pax6* morphant retinas (A, C). However, no TUNEL-positive nuclei were observed in the INL of either the control or *pax6* morphant retinas. The scale bar in panel A represents 25 microns and is the same for panels B–D. GCL, ganglion cell layer; INL, inner nuclear cell layer; ONL, outer nuclear layer.

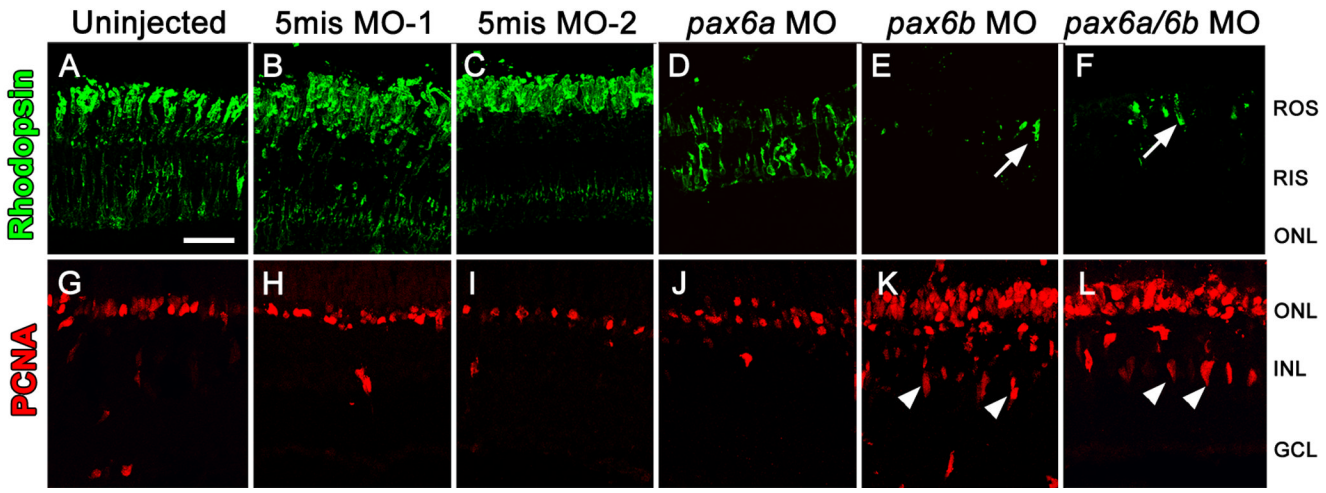

Figure 6. Rod precursor proliferation is independent of Pax6

Dark-adapted adult *albino* zebrafish were separated into three control groups, either uninjected or injected and electroporated with one of two 5-base mismatch control morpholinos (A–C and G–I), and three experimental groups, injected and electroporated with anti-*pax6a* morpholino, anti-*pax6b* morpholino, or a cocktail of both morpholinos (D–F and J–L), exposed to constant intense light for 96 hours, and then standard light for 3 days. Control retinas (A–C) possessed rhodopsin (green) labeling in newly regenerated rod photoreceptors and PCNA (red) primarily in the ONL. The *pax6a* morphant retinas exhibited visible, but relatively reduced, expression of rhodopsin that suggested minimal rod photoreceptor regeneration had occurred (D). Both the *pax6b* morphant and *pax6a/pax6b* double morphant retinas possessed only isolated rhodopsin-positive outer segments (E and F, respectively, arrows). While PCNA-positive cells in the *pax6a* morphant were largely restricted to the ONL (J), there were significantly more relative to the control retinas. The *pax6b* morphant and *pax6a/pax6b* double morphant retinas still possessed the doublets of PCNA-positive INL cells that were observed at 72 hours of constant light (Figs. 3 and 4). In addition, the *pax6b* morphant and *pax6a/pax6b* double morphant retinas contained the greatest number of PCNA-positive cells in the ONL. The scale bar in panel A represents 25 microns and is the same for panels B–L. GCL, ganglion cell layer; INL, inner nuclear cell layer; ONL, outer nuclear layer; RIS, rod inner segments; ROS, rod outer segments.

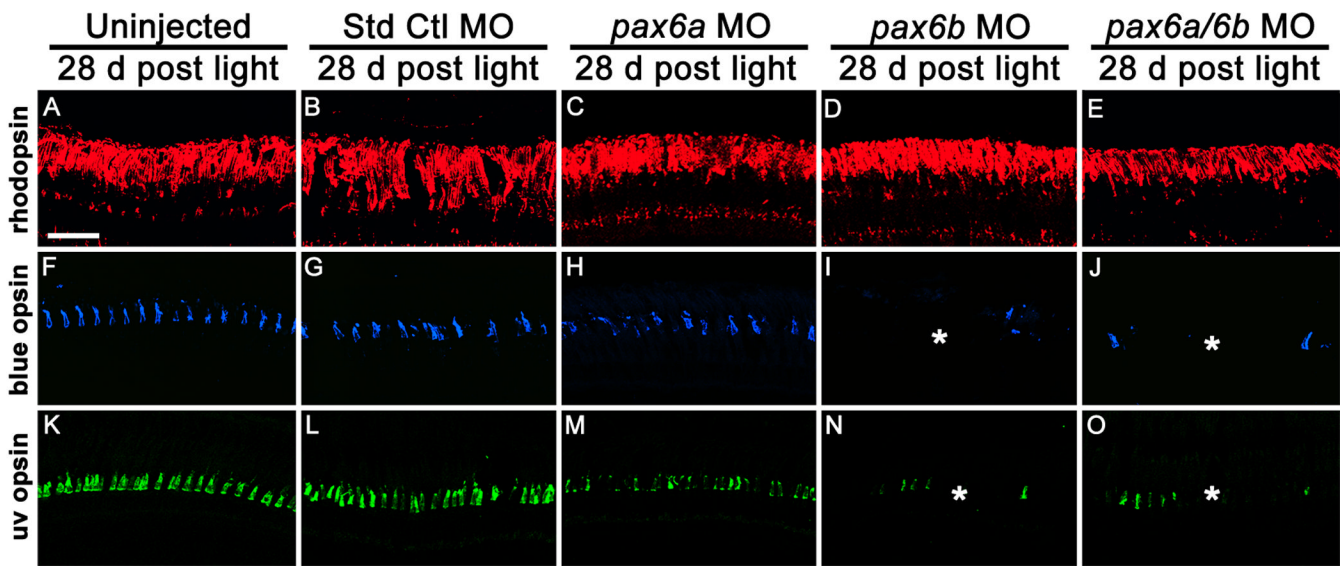

Figure 7. Pax6 is required for cone, but not rod, cell regeneration

Dark-adapted adult *albino* zebrafish were either uninjected (A, F, K) or injected and electroporated with the Standard Control morpholino (B, G, L), with anti-*pax6a* morpholino (C, H, M), anti-*pax6b* morpholino (D, I, N), or a cocktail of both morpholinos (E, J, O) and exposed to constant intense light for 96 hours. Retinas were examined 28 days following the completion of the constant light treatment. Rhodopsin immunolocalization (A–E, red) suggested that equivalent numbers of rod photoreceptors regenerated in the uninjected and morphant retinas. The *pax6b* morphant and *pax6a/pax6b* double morphant retinas contained significantly fewer long and short single cones relative to the controls, as visualized by blue opsin (F–J, blue) and UV opsin (K–O, green) immunolocalization, respectively. In contrast, the *pax6a* morphant retinas possessed an intermediate number of long and short single cones relative to the controls and the *pax6b* morphants. The scale bar in panel A represents 25 microns and is the same for panels B–O.

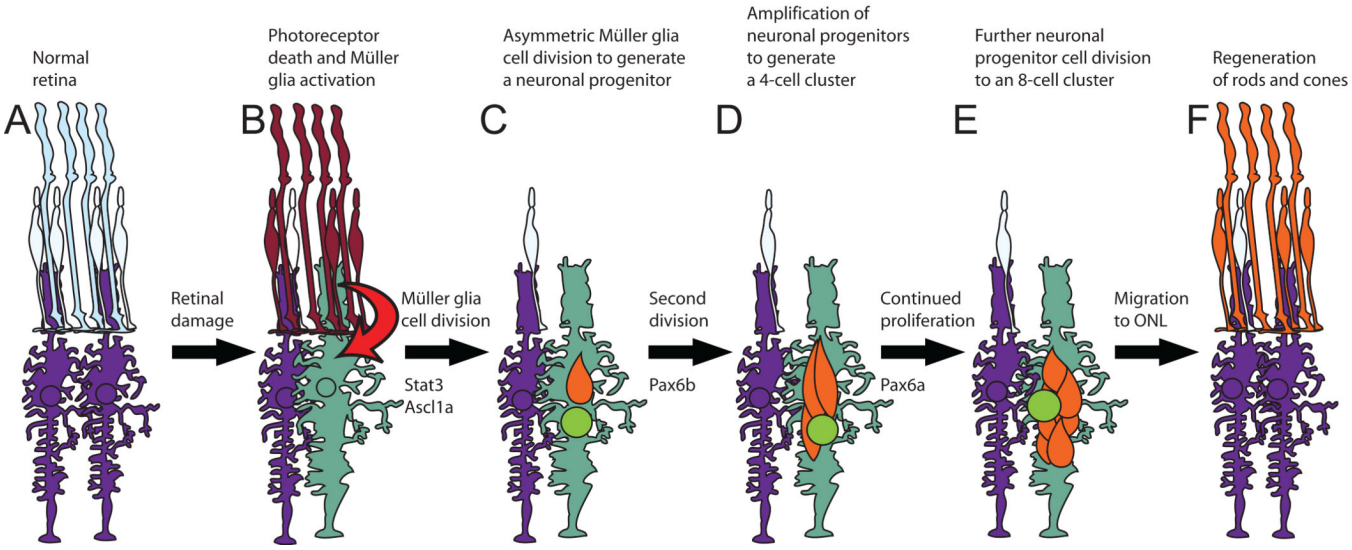

Figure 8. Model of zebrafish retinal regeneration

A. The healthy adult zebrafish retina is made up of rod (tall light blue) and cone (short light blue) photoreceptors that interdigitate with Müller glial cell processes (purple). B. Photoreceptors begin to undergo apoptosis (red) within six hours of beginning constant intense light treatment. The damaged photoreceptors signal (arrow) a subset of the Müller glial cells (green) to hypertrophy and upregulate expression of Stat3 and Ascl1a. C. By 36 hours, nearly all the rods and most of the cones are lost. The responding Müller glial cells (green) increase expression of the early response genes, such as *stat3* and *ascl1a*, and reenter the cell cycle to divide asymmetrically to produce a PCNA-positive neuronal progenitor cell (orange). D. Neuronal progenitors continue proliferating and generate the 4-cell cluster around the Müller glia. E. Neuronal progenitor cell proliferation persists until each Müller glial cell cluster contains an average of 8 nuclei. F. Neuronal progenitors migrate from the INL to the ONL, where they differentiate into newly regenerated rods and cones (orange), which are indistinguishable from the undamaged photoreceptors (light blue cone). ONL-resident rod precursor cells were ignored for simplicity.

Table 1

Quantification of Müller glia and specific neuronal classes during retinal regeneration

Dark-adapted adult *albino* zebrafish were either uninjected or injected and electroporated with: the GeneTools Standard Control morpholino; a 5-base mismatch control morpholino (5mis *pax6a* MO and 5mis *pax6b* MO), anti-*pax6a* morpholino, anti-*pax6b* morpholino, or a cocktail of both anti-*pax6* morpholinos. Expression of Müller glia and neuronal-specific cell markers were assessed after various times of constant light treatment by immunohistochemistry. Quantification of cell classes was performed on dorsal retinal sections within a 740 micron linear distance equidistant from the margin and the optic nerve. Number of retinas examined (N) and the significance level of the ANOVA analysis (p) are shown for each experiment. Standard deviations are shown in parentheses and asterisks represent data is significantly different from the controls using Bonferroni-corrected t-tests.

Average percentage of glutamine synthetase-positive Müller glia that are PCNA-positive									
Time point	N	p	Uninjected	Std. Ctl. MO	5mis *pax6a* MO	5mis *pax6b* MO	*pax6a* MO	*pax6b* MO	*pax6a/6b* MO
36 hrs light txt	6	0.792	54.6 (2.8)	48.1 (5.8)	N.A.	N.A.	51.3 (2.5)	53.2 (4.5)	49.8 (3.7)
Average number of PCNA-positive nuclei per Müller glial cluster									
Time point	N	p	Uninjected	Std. Ctl. MO	5mis *pax6a* MO	5mis *pax6b* MO	*pax6a* MO	*pax6b* MO	*pax6a/6b* MO
72 hrs light txt	6	<0.001	7.9 (0.7)	7.3 (0.5)	7.7 (0.1)	8.1 (0.3)	3.8 (0.1) *	1.9 (0.2) *	2.1 (0.2) *
Average number of BrdU-positive nuclei per Müller glial cluster									
Time point	N	p	Uninjected	Std. Ctl. MO	5mis *pax6a* MO	5mis *pax6b* MO	*pax6a* MO	*pax6b* MO	*pax6a/6b* MO
72 hrs light txt	10	<0.001	7.4 (0.6)	N.A.	8.0 (0.1)	8.1 (0.1)	4.6 (0.1) *	2.3 (0.1) *	2.0 (0.1) *
Average number of PCNA-positive nuclei in ONL									
Time point	N	p	Uninjected	Std. Ctl. MO	5mis *pax6a* MO	5mis *pax6b* MO	*pax6a* MO	*pax6b* MO	*pax6a/6b* MO
3 days post txt	6	<0.001	76.2 (4.5)	75.8 (5.6)	78.4 (5.0)	70.5 (5.6)	118.4 (20.3)	161.0 (11.4) *	158.6 (11.7) *
Average number of Müller glial cells									
Time point	N	p	Uninjected	Std. Ctl. MO	5mis *pax6a* MO	5mis *pax6b* MO	*pax6a* MO	*pax6b* MO	*pax6a/6b* MO
28 days post txt	8	0.827	70.6 (2.6)	69.1 (4.0)	N.A.	N.A.	71.4 (1.1)	68.2 (2.7)	69.0 (1.8)
Average number of ONL rod photoreceptor nuclei									
Time point	N	p	Uninjected	Std. Ctl. MO	5mis *pax6a* MO	5mis *pax6b* MO	*pax6a* MO	*pax6b* MO	*pax6a/6b* MO
28 days post txt	8	0.845	315.8 (12.0)	307.6 (12.4)	335.4 (12.7)	308.5 (11.0)	318.4 (16.3)	322.2 (17.5)	313.6 (16.4)
Average number of long single cone cells									

Time point	N	p	Uninjected	Std. Ctl. MO	5mis *pax6a* MO	5mis *pax6b* MO	*pax6a* MO	*pax6b* MO	*pax6a/6b* MO
28 days post txt	8	<0.001	49.2 (5.1)	48.2 (4.5)	50.2 (4.8)	48.4 (5.5)	34.8 (2.3)	20.8 (2.8) *	19.0 (1.9) *